IEEE/CSC & ESAS European Superconductivity News Forum (ESNF), No. 15, January 2011
The published version of this manuscript appeared in *IEEE Transactions on Applied Superconductivity* **21**, Issue 3, 871 - 874 (2011)

Two Level System Loss in Superconducting Microwave Resonators

David P. Pappas, Senior *Member IEEE*, Michael R. Vissers, David S. Wisbey, Jeffrey S. Kline and Jiansong Gao

***Abstract*—High quality factor, i.e. low loss, microwave resonators are important for quantum information storage and addressing. In this work we study the resonance frequency and loss in superconducting coplanar waveguide resonators as a function of power and temperature. We find that there is increased loss at low power and low temperature. The increased loss is attributed to the existence of two-level systems (TLS) at the surfaces, interfaces, and in the bulk of insulators deposited on the structures. We show that both the temperature dependence of the resonant frequency and the power dependence of the loss can be used to find the TLS contribution to the loss. The TLS intrinsic loss tangent derived from the frequency shift data at high power is shown to agree well with the direct loss measurement at low power. The former allows for a relatively fast measurement of the TLS loss. As an example, we measure the properties of amorphous AlO_X deposited on the resonators and find a TLS loss tangent of 1 x 10^{-3}.**

***Index Terms*—Two level system dielectric loss, superconducting resonators, low temperature physics**

I. INTRODUCTION

Superconducting resonant circuits have shown significant promise in the field of quantum computing [1]. However, short lifetimes of the devices due to anomalously high loss at very low powers and temperatures have been a severe impediment to further progress in this field. It has been shown that the most significant loss mechanism in this regime is due to unsaturated two-level systems (TLS) [2-8]. Since the early observations and explanation of this effect [9], the study of TLS has given insight into a rich variety of quantum mechanical and statistical phenomena [10]. These early studies focused on the evaluation of loss in glasses such as SiO_X and GeO_X. With the combination of modern superconducting circuits, state-of-the-art lithography techniques, and alternative dielectric and tunneling materials such as SiN_X and AlO_X, it has become increasingly important to rapidly evaluate the TLS loss in a variety of amorphous materials.

In this work, we demonstrate the correspondence of measuring the intrinsic TLS loss tangent, δ_{TLS}^0, using the loss vs. power and the resonant frequency shift vs. temperature for superconducting resonators in the 1-10 GHz regime. The first method requires many measurement averages and a relatively long measurement time to reduce the fit uncertainty due to the low signal-to-noise ratio at low power. The advantage of using the second method, i.e. Δf_r vs. T, is that it can be performed at relatively high powers, where it takes much less time to get good statistics for the resonant frequency.

Manuscript received 3 August 2010. This work was supported in part by the U.S. Department of Commerce under Grant BS123456 (sponsor and financial support acknowledgment goes here).

David P. Pappas, Michael Vissers, David S. Wisbey, Jeffrey S. Kline, and Jiansong Gao are with the National Institute of Standards and Technology, Boulder, CO 80305 USA (corresponding author phone: 303-497-3374; e-mail: David.Pappas@boulder.nist.gov). This work is a contribution of the U.S. Government, not subject to copyright.

II. BACKGROUND

The underlying physics of microwave loss due to TLS is well understood [10, 11]. However, we give a brief summary of the theoretical treatment, recently given by Gao [12] and originally derived by Hunklinger [13], in order to show the equivalence between loss measurements at low power and the frequency shifts at high power. These two are both driven by the change in the dielectric function, ϵ, due to the resonant response of an ensemble of TLS in a the microwave field. The microscopic model for these is a polar molecule, e.g. OH^-, with a precessing electric dipole moment, $\vec{D} = d\hat{d}$, in the applied electric field, $\vec{E} = E\hat{e}$. They contribute to ϵ through the susceptibility tensor, $\bar{\bar{\chi}}$, as

$$\epsilon_{TLS}(\omega) = \iiint \hat{e} \cdot \bar{\bar{\chi}}_{res} \cdot \hat{e} \, \frac{P}{\Delta_0} d\Delta d\Delta_0 d\hat{d} \quad (1a)$$

where P is the density of states, Δ is the TLS energy asymmetry matrix element, Δ_0 is the tunneling matrix element, and $\hat{e}$ is the electric field orientation. After a change of variables and integrating over $\hat{d}$ and Δ_0, (1) can be reduced to an energy integral,

$$\epsilon_{TLS}(\omega) = \epsilon' - i\epsilon'' = \frac{Pd^2}{3\hbar} \int_0^{\varepsilon_{max}} \chi_{res}(\omega) d\varepsilon. \quad (1b)$$

The real and imaginary parts of the TLS contribution to the dielectric correspond to the resonant frequency shift, Δf_r, and the internal loss, $\frac{1}{Q_i}$, of the resonator. In this equation, the susceptibility dependence on frequency, ω, can be decomposed into three parts:

$$\chi_{res}(\omega) = \left[\tanh\left(\frac{\varepsilon}{2kT}\right)\right] \quad (2a)$$

$$\times \left[\frac{1}{(\omega_\varepsilon - \omega) + iT_2^{-1}}\right] \quad (2b)$$

$$\times \left[\frac{1+(\omega_\varepsilon-\omega)^2T_2^2}{1+\Omega^2T_1T_2+(\omega_\varepsilon-\omega)^2T_2^2}\right]. \quad (2c)$$

Here, $\varepsilon = \sqrt{\Delta^2 + \Delta_0^2}$ is the eigen-energy, i.e. TLS energy splitting, $\omega_\varepsilon = \varepsilon/\hbar$ is the excitation frequency for a TLS, T_2 is

the phase decoherence lifetime, T_1 the energy relaxation lifetime, and $\Omega = 2\vec{D}\cdot\vec{E}/\hbar$ is the Rabi frequency.

The first term in χ_{res}, (2a), is a weighting function. It is equal to the probability difference between the ground and excited states, $P_1 - P_2$, where $P_2 = P_1 e^{-\varepsilon/kT}$ and $P_2 + P_1 = 1$. The second term, (2b), is the single-pole response of a TLS in its ground state under the rotating wave approximation (RWA). The third term, (2c), is the power saturation factor. For weak field or large detuning, the microwave drive is unable to change the population and this factor is close to 1. For strong electric field, i.e. above the critical field defined as E_C, the TLS in resonance with the microwave drive are "saturated". They undergo rapid Rabi oscillation between the ground state and the excited state, giving reduced response (by a factor of 2(c)) to $\chi_{res}(\omega)$. In the following section we discuss the contribution of the various terms in (2) to the loss and resonant frequency of a superconducting resonator for weak and strong driving fields.

A. TLS Loss in Weak Fields

In the weak field limit ($\Omega^2 T_1 T_2 \ll 1$), the saturation factor, (2c), is close to 1. In this case, the imaginary part of (2b), when integrated over available TLS energy splittings up to the maximum excitation energy, ε_{max}, gives the internal loss, dominated in this regime by TLS loss, in the resonator as

$$\frac{1}{Q_i} = F\delta_{TLS}^0 \tanh\left(\frac{\hbar\omega}{2k_B T}\right). \quad (3)$$

Here, Q_i is the internal quality factor of the resonator, δ_{TLS}^0 is the intrinsic TLS loss tangent at zero temperature and in a weak field, $\delta_{TLS}^0 = \delta_{TLS}\left(T \ll \frac{\hbar\omega}{2k_B}, E \ll E_C\right)$, and F is the filling factor of the TLS hosting medium in the resonator. Note that the loss from (3) tracks the TLS weighting function 2(a) in this limit. This is because the imaginary part of the RWA contribution in (2b) takes a Lorentzian profile which decays rapidly for TLS that are highly detuned (off-resonance), i.e. $\mathrm{Im}\left[\frac{1}{(\omega_\varepsilon-\omega)+iT_2^{-1}}\right] \propto \frac{1}{(\omega_\varepsilon-\omega)^2}$. Therefore, only TLS that have excitation frequency close to the drive frequency (usually set to the resonant frequency, f_r, of the superconducting resonator) contribute to the loss. According to (3), it is possible to find δ_{TLS}^0 directly from resonator loss measurements carried out with E field well below E_C, which often coincides with the single photon regime. This makes experiments difficult because the signal-to-noise ratio in this regime is poor.

B. TLS Loss in Strong Fields

In the high power limit, the saturation factor, (2c), comes into play. Since the Rabi frequency is proportional to the electric field, the term $\Omega^2 T_1 T_2$ is typically cast as $(E/E_c)^2$. The saturation means that the TLS is precessing much faster than T_1 and T_2, and hence can be found 50% of the time in the ground and excited states. Therefore, it cannot absorb any more energy. The loss tangent as a function of the electric field is given by

$$\frac{1}{Q_i} = \frac{F\delta_{TLS}^0 \tanh\left(\frac{\hbar\omega}{2k_B T}\right)}{\sqrt{1+(E/E_C)^2}}. \quad (4)$$

From this we are able to fit the loss vs. power to find the TLS loss and the critical field. However, to ensure a good fit for δ_{TLS}^0, it is still necessary to take measurements both at low and high power to get a good fit. This is a time-consuming process, as the measurement sensitivity is limited by the ~4K noise temperature of the cryogenic HEMT amplifier used in the experiment, and the signal-to-noise ratio gets poorer at lower power.

C. TLS Induced Frequency Shift in Weak and Strong Field

Complementary to the loss, changes in the real part of the dielectric, ϵ', will result in a shift of the resonator center frequency, f_r. Applying the Kramers-Kroenig relationship to (3) yields the real part of the dielectric constant, which gives rise to the temperature dependent resonant frequency shift

$$\frac{f_r(T)-f_r(T=0)}{f_r} = \frac{F\delta_{TLS}^0}{\pi}\left[\mathrm{Re}\Psi\left(\frac{1}{2}+\frac{\hbar\omega}{2\pi i k_B T}\right) - \log\frac{\hbar\omega}{2\pi k_B T}\right], \quad (5)$$

where Ψ is the digamma function.

In contrast to the loss term, the real part of the RWA contribution in (2b) decays as $\mathrm{Re}\left[\frac{1}{(\omega_\varepsilon-\omega)+iT_2^{-1}}\right] \propto \frac{1}{(\omega_\varepsilon-\omega)}$ for highly detuned TLS. This results in a slow, logarithmic convergence of the integration in (1). This means that the off-resonance TLS have significant contribution to the frequency shift, while they have little contribution to the loss. As discussed earlier, these off-resonance TLS, with a very broad spectral range of energy splittings, are not saturated. Thus, the real part of the dielectric function ϵ' is almost power independent and (5) applies to both lower and high power limits.

The result is that measuring the frequency shift of a resonator at high power and fitting the f_r vs. T data to (5) turns out to be an effective method of measuring δ_{TLS}^0. Usually these measurements can be carried out at a power at least 30 dB higher than the saturation power, where the signal-to-noise ratio is much improved as compared to the loss measurements conducted below the saturation power.

In summary, the TLS theory gives two different methods to determine δ_{TLS}^0 in superconducting resonators. The first method, loss vs. power, is a direct measurement, albeit relatively time consuming. The second method, frequency shift vs. temperature, is indirect but can be done very quickly at high power. In order to compare these methods, we have prepared resonator samples with high TLS loss and measured the loss and resonant frequency over a wide range of power and temperature.

III. Experiment

A. Samples

The resonators were fabricated from a 150 nm thick Nb film grown on hydrogen terminated, intrinsic Si substrate. The coplanar waveguide (CPW) launch line and resonators were patterned using optical lithography and a reactive ion etch consisting of an SF_6 plasma at 35 W with a -50 V bias on the

substrate. For the resonator CPW geometry, we used a 3 μm wide center strip and 2 μm wide gap. Multiple ¼-wave resonators were capacitively coupled to the launch line on each die, using slightly different lengths to achieve frequency multiplexing in the 4 – 6 GHz range. This allowed us to make several independent measurements of the resonator parameters on nominally identical samples. The coupling of the launch to the various resonators, Q_c, was also varied over a wide range, from 10k to 500k, so that we could always get close to the internal quality factor of the resonator, Q_i. This gives more confidence in the measurements.

The chip is laid out with the launch line along the center and resonators on either side. This allowed us to deposit the material under test on one side, leaving the resonators on the other side uncovered to serve as references. A Ta contact mask was used to protect the reference resonators.

In this study we chose aluminum oxide, AlO_X, as the test material because it is used as the barrier material in most superconducting tunnel junctions in practical applications. The films, 480 nm thick, were deposited at room temperature onto the sample using Al evaporation in a reactive oxygen atmosphere.

B. Measurements

An adiabatic demagnetization refrigerator (ADR) was used to conduct the low temperature measurements. The base temperature of the ADR was less than 100 mK, as measured using a RuO_X sensor attached to the sample holder. The RF measurements consisted of measuring the transmission, S_{21}, using a 1 – 20 GHz vector network analyzer. The input microwave signal was attenuated by 90 dB before reaching the device. The transmitted signal was sent to the HEMT amplifier mounted on the 4K stage through an isolator and a bias tee to block the heat and noise transmitting back from the HEMT. The HEMT gave about 35-40 dB amplification over the bandwidth used. Another 30 dB of amplification was achieved with an external, room temperature amplifier. Because the ¼-wave CPW resonator is coupled to the feedline, we measure a dip in the transmitted power at the resonance frequency. The power and temperature dependence of the resonant frequency and quality factor were then measured. The measured transmission data, S_{21}, as a function of frequency, f, are fit to

$$S_{21} = ae^{-2\pi i f\tau}\left[1 - \frac{Q_r/Q_C e^{i\phi_0}}{1+2iQ_r\left(\frac{f-f_r}{f_r}\right)}\right], \qquad (6)$$

in order to find Q_C, the measured resonator quality factor, Q_r, and the resonant frequency, f_r. The parameters a, τ, and ϕ_0 account for the gain, cable delay, and rotation of the resonance circle in the complex plane. The internal loss, $\frac{1}{Q_i}$, is obtained from

$$\frac{1}{Q_i} = \frac{1}{Q_r} - \frac{1}{Q_C}. \qquad (7)$$

This equation, in combination with (6) and (4), is used in the first method of obtaining the TLS loss.

1) First Method – Loss vs. Electric Field

To measure the low field loss directly using the first method, we measured the resonator quality factor, Q_r as a function of power and calculated Q_C and Q_i using (6) and (7). The electric field was calculated using the standard formula (see Ref. [14] eq. H4) and the aspect ratio of the coplanar waveguide. Figure 1a shows the internal loss, $\frac{1}{Q_i}$ vs. field, for the AlO_X covered sample over a wide field range. At low field, the loss is essentially constant because the TLS are not yet saturated for $E<E_C$. As we go to higher power, the loss begins to decrease sharply as the TLS saturate. Ultimately, at much higher field we see the loss flattening out again. This indicates that there is a small power independent loss term that is unrelated to the TLS loss.

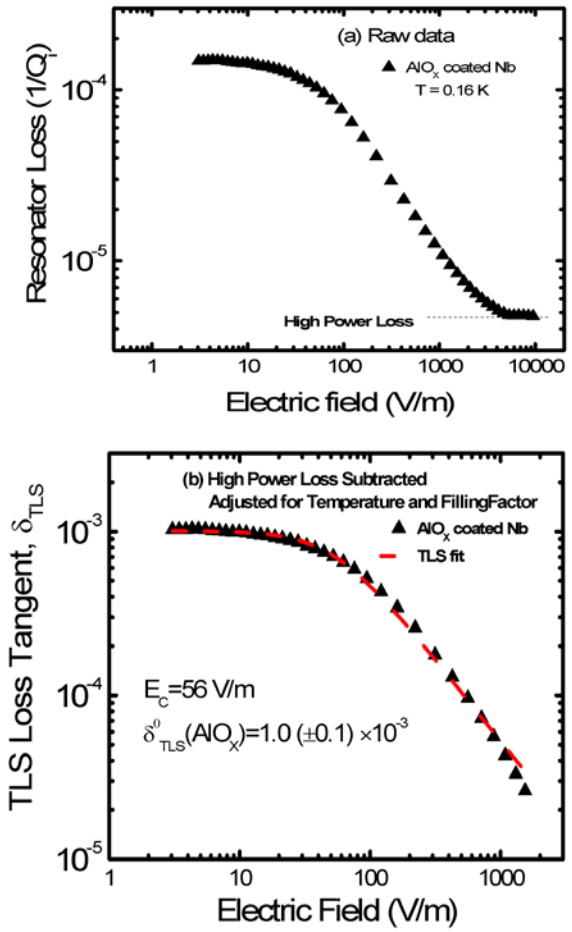

Fig. 1 (a) Top panel shows the loss in an AlO_X covered resonator (circles, f_r= 4.1288 GHz). Saturation of the loss at low field shows that we are in the single photon regime. (b) TLS loss tangent from the AlO_X covered resonator with the high power loss subtracted and adjusted for temperature (0.16 K) and filling factor, F=17% [14]. The dashed line is a fit to (4) for a TLS system with the parameters shown.

The bottom panel, Fig. 1b shows the same data with the high power background loss subtracted out, corrected for finite temperature $\left(\tanh\left(\frac{\hbar\omega}{2k_BT}\right) = 0.82\right)$, a filling factor of 0.17 [14], and fit to the expected TLS loss in (4). From this fit we find $\delta^0_{\mathrm{TLS}}(AlO_X) = 1\times10^{-3}$. For comparison, a similar analysis for the bare Nb reference resonator [15] yields $F\delta^0_{\mathrm{TLS}}(\text{bare Nb/Si}) = 5\times10^{-6}$, more than an order of magnitude lower than the AlO_X coated resonator loss.

1) Second Method – Frequency vs. Temperature

To implement the second method of obtaining $\delta_{TLS}^{0}(AlO_X)$, the resonant frequency as a function of temperature for several power levels was measured. For the AlO_X coated resonators, data is shown in Fig. 2 for fields ranging from 40 to 10,000 V/m. Each set of data was fit to (5), and the fit lines are overlaid on the data for each field value. The values of the fits for each of the fields are also shown on the right hand side of Fig. 2.

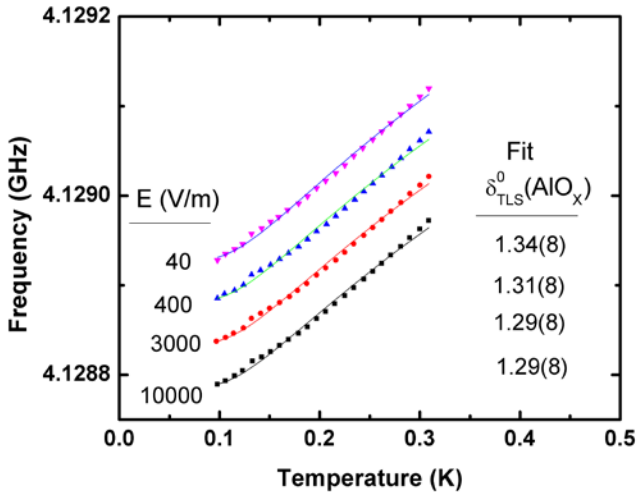

Fig. 2 Resonant frequency vs. temperature for different applied powers. The frequencies are shifted for the various powers for presentation. The data was fit for δ_{TLS}^{0} using (5) and with filling factor, F=17%. Uncertainties in the last significant figure of the fit are shown in parenthesis.

From these fits, we obtain a TLS loss of $\delta_{TLS}^{0}(AlO_X) = 1.30{\pm}0.04 \times 10^{-3}$. Similarly, using the same method, for the reference devices we find $F\delta_{TLS}^{0}(bare\ Nb/Si) = 7 \times 10^{-6}$ [15].

We see that the estimate for δ_{TLS}^{0} using this second method, f vs. T, is about 20-30% higher than the first, more direct measurement, $\frac{1}{Q_i}$ vs. E, for both the bare and AlO_X coated resonators. To understand this slight discrepancy, it should be noted that the first method only probes the TLS with excitation frequencies in the narrow frequency range near the microwave frequency ω, while the second method probes a much wider frequency range. Therefore, the former yields a "local" loss tangent and the latter yields an "average" loss tangent. In general, these do not have to be the same if the TLS density of states varies with TLS excitation frequencies.

More to the point, in the second method the high power data, taken at 10,000 V/m, can be obtained in a fraction of the time of the first method, where it is necessary to measure the saturation loss at low field. From averaging statistics, this is more than an order of magnitude speed up.

IV. Conclusion

In this work we compared two methods of determining the two-level system loss in aluminum oxide deposited on low loss, superconducting coplanar waveguides. The first method, loss vs. power, was a more direct, time consuming measurement, while the second, resonant frequency vs. temperature at high power, is indirect but more than an order of magnitude faster. The second method slightly overestimated the loss, but is useful to quickly estimate the intrinsic TLS loss tangent. This is important, for example, when there are high backgrounds of other loss or the resonance curve is distorted by other parasitic effects. .

The results also illustrate that the amorphous aluminum oxide deposited at room temperature, similar to that used for typical tunnel barriers, is inherently a high loss material. This indicates that new directions in materials for SIS junctions are important for low loss applications.

Acknowledgment

We thank Thomas Ohki, of BBN, Ben Mazin and John Martinis, of UCSB, for useful discussions during the course of this work. Danielle Braje's effort setting up the RF measurements was invaluable. This research was conducted in collaboration with BBN. It was funded in part by the Office of the Director of National Intelligence (ODNI), Intelligence Advanced Research Projects Activity (IARPA). All statements of fact, opinion or conclusions contained herein are those of the authors and should not be construed as representing the official views or policies of IARPA, ODNI, or BBN.

References

[1] J. Clarke, and F. K. Wilhelm "Superconducting quantum bits" Nature **453**, 1031 (2009).
[2] H. Wang, M. Hofheinz, J Wenner, M. Ansmann, R.C. Bialczak, M. Lenander, E. Lucero, M. , A.D. O'Connell, D. Sank, M. Weides, A.N. Cleland, and J. Martinis, Appl. Phys. Lett. **95**, 233508 (2009).
[3] J. Gao, M. Daal, A. Vayonakis, S. Kumar, J. Zmuidzinas, B. Sodoulet, B. A. Mazin, P. K. Day, H. G. Leduc, Appl. Phys. Lett. **92**, 152505 (2008)
[4] T. Lindstrom, J.E. Healey, M.S. Colclough, C.M Muirhead, and A. Ya. Tzalenchuk, Phys Rev B **80**, 132501 (2009).
[5] R. Barends, H. L. Hortensius, T. Zijlstra, J. J. A. Baselmans, S. J. C. Yates, J. R. Gao, T. M. Klapwijk, Appl. Phys. Lett. **92**, 223502 (1990).
[6] Y. Q. You, F. Nori, Physics Today, p.42 November(2005)
[7] M. Steffen, M. Ansmann, R. McDermott, N. Katz, R. C. Bialczak, E. Lucero, M. Neeley, E. M. Weig, A. N. Cleland, J. M. Martinis, Phys. Rev. Lett. **97**, 050502 (2006).
[8] P. Macha, S. H. W. van der Ploeg, G. Oelsner, E. Il'ichev, H. -G. Meyer, S. Wunsch, M. Siegel, Appl. Phys. Lett. **96**, 062503 (2010).
[9] M. von Schikfus and S. Hunklinger, J. Phys. C: Solid State Phys. **9**, L439 (1976).
[10] W. A. Phillips, Rep. Prog. Phys. 50, pp. 1657-1708 (1987).
[11] P. W. Anderson, B. I. Halperin, C. M. Varma, Philosophical Magazine **25,** 1-9 (1972).
[12] Jiansong Gao, "The physics of superconducting microwave resonators", Caltech Ph.D. thesis, (2008). http://resolver.caltech.edu/CaltechETD:etd-06092008-235549
[13] S. Hunklinger and W. Arnold, Physical Acoustics, 12, ch. 3, p. 155 Academic, New York (1976).
[14] Rainee N. Simons, "Coplanar Waveguide Circuits, Components, and Systems" Wiley Series in Microwave and Optical Engineering, Kai Chang, Series Editor (2001) by John Wiley and Sons, ISBN 0-471-16121-7.
[15] D. S. Wisbey, J. Gao, M. R. Vissers, F. C. S. da Silva, J. S. Kline, L. Vale, D. P. Pappas, Jour. Appl. Phys., in press (Oct. 2010).